Error Performance Analysis of Random Network Coded Cooperation Systems

Semiha Tedik Basaran, *Student Member, IEEE*, Selahattin Gokceli, Gunes Karabulut Kurt, *Senior Member, IEEE*, Enver Ozdemir, and Ergün Yaraneri

***Abstract*— This paper presents a framework for computing successful decoding probability of random network coding (RNC) in wireless networks. As cooperation emerges due to the naturally occurring broadcasting in wireless links, the application of RNC in wireless networks enables random network coded cooperation (RNCC). The theoretical successful decoding probability of RNCC systems is derived by obtaining the ratio of the full rank and the rank deficient matrices. The full rank condition of the global encoding matrix indicates the successful decoding of source symbols. The results of a single relay along with a relay selection scheme are also investigated. The validity of the presented theoretical expressions is demonstrated through identical simulation results. An implementation scenario is also presented to demonstrate the practical usage effectiveness of RNC in real-time applications, by using software-defined radio nodes.**

***Index Terms*— Galois fields, cooperative communication, random network coding, successful decoding probability.**

I. Introduction

CONVENTIONAL routing schemes enable only to store-and-forward the received data symbols at intermediate nodes. On the other hand, intermediate nodes also referred to as relay nodes, become smarter than their previous counterparts and they can store process and forward combinations of multiple data symbols. This technique, called network coding (NC), is proposed in [1], and it is based on the early work of Yeung about diversity coding [2]. NC provides a more efficient usage of limited communication resources such as power, bandwidth, and frequency spectrum when compared to the conventional routing schemes. Thanks to the relay nodes, transmitting the combinations of received signals by using NC increases the throughput and robustness of the wireless communication systems. NC has the potential to meet the demands of high rate applications with increasing number of users. In the early works, the error-free transmission assumption is used for NC for wire-line networks [1], [3], [4]. This assumption is not realistic for wireless networks as they are more prone to errors and erasures due to multipath fading effects of the wireless channel. Although wireless links have unfavorable error performances, they also bring along an inherent advantage as direct transmission links. Any direct transmission link between a source and a destination in addition to relay links provides a significant transmission benefit. This link supplies cooperation gain by exploiting the broadcast nature of the wireless channel [5], [6]. Hence, the implementation of NC in wireless networks should not be considered without cooperation gain between a source and destination nodes. Applying NC in wireless networks, while considering the direct transmission link, is called network coded cooperation (NCC). NCC leads to significant error performance gains when compared to pure NC due to cooperative gain [7].

In order to improve the error performance and the efficiency of resource usage of wireless network based on various resource scheduling in time or frequency, many NCC system models are proposed [8]. It is shown that, as a unified communication technique, NCC jointly exploits cooperative diversity due to direct links between source and destination nodes and provides considerable throughput advantages. The type of network code determines the performance and the throughput of the system. Linear network codes that require a centralized scheme for the particular network topology may not be suitable for wireless networks because link failure is frequently encountered in wireless networks. Another issue that needs to be addressed is the scalability problem of linear network codes for dense networks. The requirements introduced by wireless channels for dynamic and flexible schemes can be satisfied by random network coding (RNC), which is proposed as a type of linear network code [9]–[12]. RNC is a straightforward and convenient approach to represent the dynamic nature of the wireless channel, allowing decentralized controlling and providing robustness for changes in network topology.

The effectiveness of RNC is demonstrated for LTE networks in [13] and [14]. In RNC, network code coefficients are generated randomly at relay nodes without conforming to any code set for all relay nodes. The coefficients of random network codes are selected from $\mathcal{GF}(q)$, a field of size q. They are independent and identically distributed ($i.i.d.$) following uniform distribution. If the field size is sufficiently large, independent coding vectors of different relays can be obtained. The linearity property of NC is also preserved in RNC. When RNC is selected as a network code in NCC system, the term

Manuscript received July 19, 2016; revised January 30, 2017 and April 27, 2017; accepted May 2, 2017. Date of publication May 31, 2017; date of current version August 10, 2017. This work is supported by TUBITAK under Grant 113E294. The associate editor coordinating the review of this paper and approving it for publication was M. Payaró. *(Corresponding author: Semiha Tedik Basaran.)*

S. Tedik Basaran, S. Gokceli, and G. Karabulut Kurt are with the Department of Communications and Electronics Engineering, Istanbul Technical University, 34469 Istanbul, Turkey (e-mail: tedik@itu.edu.tr; gokcelis@itu.edu.tr; gkurt@itu.edu.tr).

E. Ozdemir is with the Institute of Informatics, Istanbul Technical University, 34469 Istanbul, Turkey (e-mail: ozdemiren@itu.edu.tr).

E. Yaraneri is with the Department of Mathematics, Istanbul Technical University, 34469 Istanbul, Turkey (e-mail: yaraneri@itu.edu.tr).

Color versions of one or more of the figures in this paper are available online at http://ieeexplore.ieee.org.

Digital Object Identifier 10.1109/TWC.2017.2708702

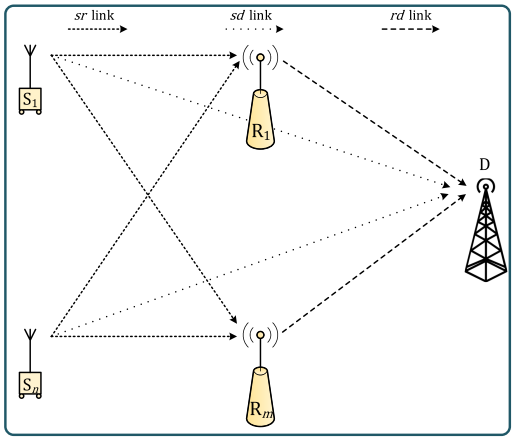

Fig. 1. The network model with m number of relay nodes, n number of source nodes, and one destination node. Relay nodes perform random network coding on detected source symbols.

of random network coded cooperation (RNCC) is used to define the system. A multi-source multi-relay RNCC system is depicted in Fig. 1 with m number of relay nodes and n number of source nodes which are denoted by R_i and S_j with $i = 1, \ldots, m$ and $j = 1, \ldots, n$. For the RNCC system it is assumed that there is only one target node denoted by D. There are three types of link as source to relay, source to destination and relay to destination which are represented by sr, sd, and rd, respectively.

In this paper, we derive the theoretical successful decoding probability of RNCC which fills the void in the NCC literature. Our main contributions are listed as:

- We introduce a generalized framework to analyze wireless RNCC by using rank-based detector.
- We propose a method to calculate the successful decoding probability of RNCC for generalized multi-source multi-relay topologies.
- We provide the successful decoding probability expression of single relay and relay selection cases with reduced complexity due to the simplicity of network according to multi-relay case.
- We validate the theoretical results with simulations to ensure the reliability of derivations.
- To the best of our knowledge, RNC is implemented the first time in our study by using software defined radio (SDR) nodes.

The rest of the paper is organized as follows. The details of system model consisting of channel and network models are given in Section II. The framework of calculation of successful decoding probability with theoretical derivations is expressed in Section III. In Section IV, the simulation and compatible theoretical results are presented with detailed comments. The implementation details and measurement results are given in the following part, Section V. The main outcomes and summarized contributions of our works can be found in Section VI.

A. Related Works

Although there are related studies in the literature [15]–[23], a comprehensive approach for calculating the successful decoding probability of RNCC under wireless channel conditions remains an open issue. The exact decoding probability of RNC is derived by using q-binomial coefficients (Gauss coefficients) to simplify decoding probability expressions according to field size q [15]. The decoding probability analysis of RNC is given for erasure channels [16], without taking into account the different effects of high outage cases. However, this missing point has a significant effect on the decoding probability of RNC. The authors do not consider the effect of various partitions of the number of failed source to relay links. Hence, the theoretical decoding probability expression of RNC given in [16] is an approximation of the exact expression. Another work on erasure channels about RNC is [17], in which there is a constraint that the coding coefficients are selected in $\mathcal{GF}(q)\backslash\{0\}$. The tightness of the presented bounds is demonstrated with simulation results of RNCC. Seong and Lee [18] propose an analysis model for RNCC to determine the bounds of decoding probability. In [17] and [18] the bounds of theoretical decoding probability are expressed tightly in a limited region independent of q. In addition to this constraint, they also consider the homogenized networks in which signal to noise ratio (SNR) values of direct and cooperation links are accepted as the same. However, this is not generally probable for wireless links when calculating the upper bounds of decoding probability. Hence, [18] does not provide the closed form expressions for generalized wireless channel conditions. On the other hand, tight bounds (upper and lower) of RNC which coding coefficients selected from $\mathcal{GF}(q)\backslash\{0\}$, for multi-source multi-relay scheme are presented [19] without considering source to destination links. An optimized framework is proposed to minimize overhearing probability while guaranteeing successful decoding at legitimate user by transmitting random network coded symbols from a source node over erasure channels [20]. Predefined delay and reliability constraints are used when performing simulations and obtaining theoretical derivations. The exact decoding probability expressions of the rank-based detector are given for RNC in the field $\mathcal{GF}(2)$ by considering erasure patterns [22]. The decoding probability results of RNCC is presented by using coding at both of source and relay nodes to assist a single relay node [23]. They also give the tight upper bounds of the proposed system setup.

II. System Model

We consider an RNCC system with n source nodes, m relay nodes and one destination node as shown in Fig. 1. The details of the system about channel and network models are given in the following subsections.

A. Channel Model

The transmission process of RNCC has been completed in two orthogonal transmission phases as broadcast and relaying. In the broadcast phase, source nodes transmit their information-bearing signals to relay and destination nodes. The received signals by relay nodes are given as:

$$y_{s_j r_i} = h_{s_j r_i} x_j + w_{s_j r_i}, \tag{1}$$

where x_j denotes the modulated signal of S_j in the broadcast phase. The gain of the channel between S_j and R_i is indicated by $h_{s_j r_i}$ and the additive white Gaussian noise (AWGN) component at R_i is indicated by $w_{s_j r_i}$ for x_j. The transmitted signals, x_j are received by destination at the same time due to the inherent wireless channel nature. The received signals at the destination are equal to:

$$y_{s_j d} = h_{s_j d} x_j + w_{s_j d}, \tag{2}$$

where $h_{s_j d}$ and $w_{s_j d}$ denote the gain of the channel between S_j and D and the AWGN component at D. Following the broadcast phase, each relay node detects the received signals and encodes these signals. The encoded symbol of R_i can be calculated as a summation in $\mathcal{GF}(q)$ which can be given as:

$$z_i = \sum_{j=1}^{n} \alpha_{ij} \tilde{x}_{ij}, \tag{3}$$

where $\tilde{x}_{ij}$ denotes the detected version of the modulated signal x_j at R_i. Relay nodes employ RNC where the coding coefficients, α_{ij}, are selected $i.i.d.$ following uniform distribution from a finite field, $\mathcal{GF}(q)$, (also denoted by $\mathbb{F}_q$) [12]. Hence, α_{ij} can uniformly and randomly take the values from 0 to $q-1$. The field size q is an important design parameter which determines the decoding performance of RNCC. After generating network coded symbols, relay nodes perform transmission of the symbols in orthogonal resource blocks to avoid generating interference at the destination. Relay nodes forward z_i symbols to destination nodes in the relaying phase. The received signal of R_i at destination is given as:

$$y_{r_i d} = h_{r_i d} z_i + w_{r_i d}, \tag{4}$$

where $h_{r_i d}$ and $w_{r_i d}$ indicate the channel gain between R_i and D and AWGN component at D. At the end of the transmission process, destination node tries to decode received packets by performing rank based detector with using transmission matrix [12]. Some packets may not be received at R_i and/or destination due to the wireless impairments, hence outage events are considered in the calculation of the successful decoding probability of the RNCC.

Outage probability is a meaningful metric to measure the quality of transmission which defines the connection status of any transmission link. The outage probability of link u is determined according to:

$$\phi_u = \mathbb{P}\left\{\log\left(1 + |h_u|^2 \gamma_u\right) < \mathcal{R}_u\right\}, \tag{5}$$

where h_u and γ_u define the gain and SNR of link u with $u = sd,\ sr,\ rd$. $\mathcal{R}_u$ indicates the target transmission rate of link u to avoid outage status. The expression in (5) can be simplified as:

$$\phi_u = \mathbb{P}\left\{|h_u|^2 < \frac{2^{\mathcal{R}_u} - 1}{\gamma_u}\right\}. \tag{6}$$

We define a new random variable as $\mathcal{G} = |h_u|^2$, hence the expression of the right hand side of (6) represents the cumulative distribution function (CDF) of g_u which is denoted by $\mathcal{F}_{\mathcal{G}}(g_u)$ where $g_u = \left(2^{\mathcal{R}_u} - 1\right)/\gamma_u$. The outage probability of the transmission link u can be easily defined through CDF expression as $\phi_u = \mathcal{F}_{\mathcal{G}}(g_u)$. For Rayleigh block fading channels, the expression in (5) is transformed into:

$$\phi_u = 1 - \exp\left(-\left(2^{R_u} - 1\right)/\gamma_u\right), \tag{7}$$

by using the information about the exponential distribution of $\mathcal{G}$. Hence, we use the relation between SNR and the outage probability for the derivation of the decoding probability of RNCC.

To simplify the notation, we assume that there are three types of channels as source-destination (sd), source-relay (sr) and relay-destination (rd). All links of each channel type have the same outage level with $\phi_{s_j d} = \phi_{sd}$, $\phi_{s_j r} = \phi_{sr}$, $\phi_{r_i d} = \phi_{rd}$. The outage probability of any sd (sr) link is indicated by ϕ_{sd} (ϕ_{sr}) in the broadcast phase. ϕ_{rd} denotes the outage probability of any rd link in the relaying phase.

B. Network Model

As mentioned above, a cooperative communication set-up is composed of two phases as broadcast and relaying between a source node and a destination node [24]. In the broadcast phase, source nodes transmit information-bearing signals to relay and destination nodes by using orthogonal radio resources. Both relay and destination nodes can detect transmitted packets due to the broadcast nature of the wireless communication channel. Relay nodes detect the received symbols in the first phase. In the relaying phase, each relay node encodes the sources' packets using a network code. This network code can be selected from a predetermined code or generated randomly. Maximum distance separable codes are preferred to yield Singleton bound by considering Hamming distance among codewords. On the other hand, RNC satisfies dynamic network requirements due to its decentralized control nature. Hence, RNC is more suitable for wireless networks when compared to any predetermined coding scheme.

RNCC system's global encoding matrix $\mathbf{Z} \in \mathbb{F}_q^{(n+m)\times n}$ is defined as:

$$\mathbf{Z} := \begin{bmatrix} \mathbf{D} \\ \hline \mathbf{R} \end{bmatrix} = \left[\begin{array}{cccc|ccc} d_1 & 0 & \cdots & 0 & \alpha_{11} & \cdots & \alpha_{m1} \\ 0 & d_2 & \cdots & 0 & \alpha_{12} & \cdots & \alpha_{m2} \\ \vdots & \vdots & \ddots & \vdots & \vdots & \ddots & \vdots \\ 0 & 0 & \cdots & d_n & \alpha_{1n} & \cdots & \alpha_{mn} \end{array}\right]^T, \tag{8}$$

where the first n entries of $\mathbf{Z}$ form an $n \times n$ diagonal submatrix, corresponding to the direct transmission of sd links in broadcasting phase [24]. The remaining entries correspond to the random network coded packets transmitted by relay nodes. If the link between S_j and D is in outage, d_j is equal to zero, otherwise, it is equal to 1 in $\mathcal{GF}(q)$. We assume that relay nodes which successfully decode at least one packet from n source nodes are allowed to participate in the relaying phase using RNC, and we assume that at most one link from source to each relay node fails due to preserving network coding scheme.

Example 1: We give an example of RNCC system with $n = 3$, $m = 4$ to explain the global encoding matrix, $\mathbf{Z}$. After completion of two transmission phases, destination node

requires $\mathbf{Z}$ to obtain source symbols correctly. For instance, the global encoding matrix of this system in error-free case is given as:

$$\mathbf{Z} = \left[\begin{array}{ccc|cccc} 1 & 0 & 0 & \alpha_{11} & \alpha_{21} & \alpha_{31} & \alpha_{41} \\ 0 & 1 & 0 & \alpha_{12} & \alpha_{22} & \alpha_{32} & \alpha_{42} \\ 0 & 0 & 1 & \alpha_{13} & \alpha_{23} & \alpha_{33} & \alpha_{43} \end{array}\right]^T. \quad (9)$$

As frequently used in RNC literature [10]–[12], we assume that the encoding matrix is available at destination. This approach is called coherent detection. On the other hand, if destination has no prior knowledge about the encoding matrix, it tries to obtain the coefficients through different ways, such as transmission of pilot symbols from relay nodes by using the coefficients or placing the coefficients at the beginning of each transmitted packet at relay nodes. This strategy is referred to as non-coherent NC [9], [25], [26]. Consequently, the destination node needs to have the knowledge about the encoding matrix in some way to successfully decode the received symbols. After that, the knowledge about coding matrix simplifies the decoding procedure at the destination node. Hence Gauss-Jordan elimination method can be used to decode the received symbols over $\mathcal{GF}(q)$ [12]. If the destination node has minimum n number of orthogonal code vectors, it can obtain all source symbols. The number of orthogonal code vectors can be calculated as the rank of a given encoding matrix. The used detector, referred to as rank-based detector, checks whether the rank condition is met to calculate the successful decoding probability.

III. Decoding Probability Analysis of RNCC

The theoretical decoding probability expressions of RNCC system will be derived by considering the destructive effects of wireless channels. The field size q must be taken into account as another design parameter which affects the decoding probability performance of RNCC. The rank-based detector, a frequently preferred technique in the RNCC literature, will be used as the detector at the destination node.

A. Link Outages

The effects of outage status of each type of transmission links (sd, sr, and rd) on decoding probability performance of RNCC are different. Hence, they need to be individually considered. First, we investigate the effect of outage situation of sd links. The probability of k number of sd links in outage is given by:

$$P_{sd}(k) = \binom{n}{k} \phi_{sd}^{k} (1-\phi_{sd})^{n-k}, \quad (10)$$

where $n-k$ number of sd links are in non-outage state. The sd links in outage results in zero elements in the diagonal of the upper matrix of $\mathbf{Z}$. If there is no outage sd links, destination node accurately decodes the received signals without the requirement of any encoded symbols. On the other hand, if any sd link is in outage, destination node requires encoded symbols to decode source symbols.

The probability that l links fail of rd links can be calculated as:

$$P_{rd}(l) = \binom{m}{l} \phi_{rd}^{l} (1-\phi_{rd})^{m-l}, \quad (11)$$

where $m-l$ number of rd links are available in the system. There might be sr link outages in the system in addition to sd and rd link failures. The occurrence probability of t number of failed sr links will be given in the next section.

Outage status of j^{th} sd link is represented by $d_j = 0$, where the rank of $\mathbf{Z}$ may be decreased by one. This reduction of the rank causes performance degradation in the rank-based detector. If any rd link is in outage, destination loses the related relay's symbol that contains combination of all source symbols. Hence, the corresponding row of $\mathbf{Z}$ is set to all zeros. In the case of a link failure in sr, the corresponding source signal can not be used by the corresponding relay node in the encoding process, and so only the corresponding entry in the matrix $\mathbf{Z}$ is deleted.

$\mathbf{Z}$ can be simplified by using the definitions above and the information about k and l, which represent the number of outage links. We may assume that the failed sd (rd) links are the first k (the last l) number of sd (rd) links. That is, the first k diagonal entries of $\mathbf{D}$ are zero, the last l rows of $\mathbf{R}$ are zero. The updated version of $\mathbf{Z}$ is represented by $\mathbf{Z}'$, and it is used to simplify the derivations of the successful decoding probability of RNCC. Hence, the reduced encoding matrix is determined as the $(n+m) \times n$ block matrix:

$$\mathbf{Z}' = \left[\begin{array}{c|c} 0 & 0 \\ \hline 0 & \mathbf{I_{n-k}} \\ \hline \mathbf{B} & \mathbf{C} \\ \hline 0 & 0 \end{array}\right], \quad (12)$$

where $\mathbf{B}$ is a $(m-l) \times k$ matrix, $\mathbf{C}$ is a $(m-l) \times (n-k)$ matrix, $\mathbf{I_{n-k}}$ is the $(n-k) \times (n-k)$ identity matrix, and the zeros appearing are zero matrices of appropriate sizes. The rank of the last $n-k$ columns of $\mathbf{Z}'$ is equal to $n-k$ due to the identity matrix, indicated by $\mathbf{I_{n-k}}$, of size $n-k$ in $\mathbf{Z}'$. Hence the probability of $\mathbf{Z}$ has full rank n is the same as the probability of $\mathbf{B}$ has rank k, because we have the following expression:

$$\text{rank}(\mathbf{Z}') = \text{rank}(\mathbf{B}) + (n-k). \quad (13)$$

The successful decoding probability of RNCC system, which is the probability of $\mathbf{Z}$ having full rank, is equal to the probability of $\mathbf{B}$ having rank k. Hence, we continue by considering only $\mathbf{B}$ matrix to derive the successful decoding probability of RNCC to reduce the computational complexity of the derivations. Hence, sr link outages must be considered for $\mathbf{B}$ matrix instead of $\mathbf{Z}$.

If the link between S_j to R_i is in outage, then the $(i, j)^{\text{th}}$ entry of the bottom matrix of $\mathbf{Z}$ is forced to be zero. We assume that for each relay node at most one of the n incoming links from sources is in outage. Therefore, t links fail from sources to relays means that exactly t relays loose a packet, and so exactly t rows of the bottom matrix of $\mathbf{Z}$ have precisely one entry forced to be zero with probability ϕ_{sr}. Note that if an rd link fails then we assume that there is no source which fails when transmitting data to that relay. That is, we

assume that if a row of $\mathbf{Z}$ consists entirely of zeros then that row does not contain any entry which is forced to be zero. We continue with the reduced matrix $\mathbf{B}$ to obtain decoding probability. The outage probability of an sr link is equal to $k\phi_{sr}/n$ since $\mathbf{B}$ has k columns. The probability that t links fail from sources to relays is given by:

$$P_{sr}(t) = \binom{m-l}{t}\left(\frac{k\phi_{sr}}{n}\right)^t\left(1-\left(\frac{k\phi_{sr}}{n}\right)\right)^{m-l-t}, \quad (14)$$

where the number of rows and columns of $\mathbf{B}$ matrix are equal to $m-l$ and k, respectively.

Example 2: We continue with the example of encoding matrix, $\mathbf{Z}$ is given in (9). The parameters are given as $k=2$, $l=1$, and $t=1$ are related to channel conditions. The reduced encoding matrix of destination node is given as:

$$\mathbf{Z}' = \left[\begin{array}{ccc|ccc|c} \boxed{0} & 0 & 0 & \alpha_{11} & \alpha_{21} & \alpha_{31} & \boxed{0} \\ 0 & \boxed{0} & 0 & \alpha_{12} & \alpha_{22} & \alpha_{32} & 0 \\ 0 & 0 & 1 & \alpha_{13} & \boxed{0} & \alpha_{33} & 0 \end{array}\right]^T, \quad (15)$$

where the dashed, dotted and solid boxes represent the sd, sr and rd link failures, respectively.

B. Calculation of Conditional Successful Decoding Probability

We determined the probability of the number of link failures of sd, sr, and rd in the previous subsection. We, now, consider a particular configuration of k out of n sources for which data transmission from these k sources to a destination fail, a particular configuration of l out of m relays for which data transmission from these l relays to the destination fail and a particular configuration of t out of m relays for which data transmission from sources to these relays fail. We let $\mathcal{A}_{klt}$ be the set of block matrices $\mathbf{Z}$ for which the entries d_j of $\mathbf{D}$ corresponding to these k sources are zero, the rows of $\mathbf{R}$ corresponding to these l relays consist entirely of zeros, and exactly one entry in each of t rows of $\mathbf{R}$ corresponding to these t sources is forced to be zero. We also let $\mathcal{B}_{klt}$ be the set of matrices in $\mathcal{A}_{klt}$ that have full rank n. For this particular configurations of k sources, l relays, and t sources, the probability of successful decoding at the destination is equal to the ratio $\frac{|\mathcal{B}_{klt}|}{|\mathcal{A}_{klt}|}$, where $|\cdot|$ indicates the cardinality operator.

As permuting rows do not change the rank of any matrix, the probability of successful decoding when k sources to destination fail and l relays to destination fail, and t sources to relays fail, do not depend on the particular configurations of k, l, and t. Thus, the conditional successful decoding probability for a particular configuration is given by:

$$P(d\ |k\ sd,\ l\ rd,\ t\ sr) = \frac{|\mathcal{B}_{klt}|}{|\mathcal{A}_{klt}|}. \quad (16)$$

C. Counting Full Rank and Rank Deficient Matrices

In order to calculate the successful decoding probability of RNCC, we need to consider all type of link outages and all configurations. Therefore, the successful decoding probability at the destination node is computed through the following expression:

$$P_d = \sum_k\sum_l\sum_t P(d\ |k\ sd,\ l\ rd,\ t\ sr)P_{sd}(k)P_{rd}(l)P_{sr}(t). \quad (17)$$

The conditional successful decoding probability of RNCC is given as:

$$P(d\ |k\ sd,\ l\ rd,\ t\ sr) = \sum \frac{1}{c_{k,l,t}}\frac{|\mathcal{B}_{klt}|}{|\mathcal{A}_{klt}|}, \quad (18)$$

where the sum ranges over all possible configurations of k, l, and t. $c_{k,l,t}$ represents the number of all possible configurations of k, l, and t.

It is clear that $c_{k,l,t} = c_k c_l c_t$ where c_k, c_l, and c_t are the respective numbers of all possible configurations of k, l, and t satisfying the required conditions. We now target to count of c_t of all possible configurations of t when the numbers k, l, and t are fixed and when the configurations of k and l are fixed. Let t which is the number of relays to which data transformations from sources fail, be a fixed number. For any j, we let x_j be the number of entries in the j^{th} column of $\mathbf{R}$ which are forced to be zero. We obtain an equation:

$$x_1 + x_2 + \cdots + x_n = t, \quad (19)$$

where x_i are non-negative integers. For a fixed solution $x_1, x_2 \ldots x_n$ of (19), $C(x_1, x_2, \ldots, x_n)$ is the number of $m \times n$ matrices $\mathbf{R}$ whose j^{th} column contains x_j number of forced zero entries. It may be calculated as follows: Each column has m entries and so x_1 zeros in the first column of $\mathbf{R}$ may be distributed in $\binom{m}{x_1}$ ways. As each row of $\mathbf{R}$ can have at most one forced zero entry, x_2 zeros in the second column of $\mathbf{R}$ should be distributed to $m-x_1$ rows, which may be done in $\binom{m-x_1}{x_2}$ ways. Continuing in this manner we observe that

$$\begin{aligned} C(x_1, x_2, \ldots, x_n) &= \binom{m}{x_1}\binom{m-x_1}{x_2}\binom{m-(x_1+x_2)}{x_3} \\ &\quad \times \binom{m-(x_1+x_2+\cdots+x_{n-1})}{x_n} \\ &= \frac{m!}{x_1!x_2!\cdots x_m!(m-t)!}. \end{aligned} \quad (20)$$

Therefore, the number of all possible configurations of t can be defined as:

$$c_t = \sum C(x_1, x_2, \ldots, x_n), \quad (21)$$

where the sum ranges over all nonnegative integer solutions of (19). The above sum expressing c_t has $\binom{n+t-1}{t}$ summands, which is the number of nonnegative integer solutions of the (19).

The set of all permutations of a finite set with n elements forms the symmetric group S_n. Details about definitions of symmetric groups are available in [27]. In our case, by permuting the indices of a solution, the symmetric group S_n acts on the set of nonnegative integer solutions of (19). This action corresponds the permutations of the columns of $\mathbf{R}$ and hence does not change the rank. To be more precise, by

permuting columns of the symmetric group S_n acts on the set $\left\{\mathcal{M}_{x_1,x_2,\ldots,x_n}\right\}$ where x_i ranges over all non-negative integer solutions of (19) and $\mathcal{M}_{x_1,x_2,\ldots,x_n}$ is the set of all $m\times n$ matrices each of whose j^{th} column contains x_j forced zero entries and whose rows have at most one forced zero. Note that the set $\bigcup \mathcal{M}_{x_1,x_2,\ldots,x_n}$, where x_i ranges over all nonnegative integer solutions of the (19), consists of all possible configurations of t and note also that:

$$|\mathcal{M}_{x_1,x_2,\ldots,x_n}| = C(x_1, x_2, \ldots, x_n). \tag{22}$$

Suppose that the action of S_n on the set of nonnegative integer solutions of (19) transforms the solution z_i to the solution $\overline{z}_i$. Then the corresponding action on the set $\left\{\mathcal{M}_{x_1,x_2,\ldots,x_n}\right\}$ transforms the set $\mathcal{M}_{z_1,z_2,\ldots,z_n}$ to the set $\mathcal{M}_{\overline{z}_1,\overline{z}_2,\ldots,\overline{z}_n}$. Choosing arbitrary matrices $\mathbf{M} \in \mathcal{M}_{z_1,z_2,\ldots,z_n}$ and $\overline{\mathbf{M}} \in \mathcal{M}_{\overline{z}_1,\overline{z}_2,\ldots,\overline{z}_n}$, we have two configurations of t corresponding to $\mathbf{M}$ and $\overline{\mathbf{M}}$. As permuting rows and columns do not change the rank, the numbers $|\mathcal{A}_{klt}|$ and $|\mathcal{B}_{klt}|$ in two configurations of t corresponding to $\mathbf{M}$ and $\overline{\mathbf{M}}$ are the same. Therefore, for a fixed t, instead of summing probabilities in each of all possible configurations of t, we may take an arbitrary configuration in any matrix lying in any set in each orbit of the action of S_n on the set $\left\{\mathcal{M}_{x_1,x_2,\ldots,x_n}\right\}$. The last sum becomes:

$$P(d|k\ sd,\ l\ rd,\ t\ sr) = \sum_{k,l} \frac{1}{c_k c_l} \sum_{t} \frac{C(x_1, x_2, \ldots, x_n) o_t}{c_t} \frac{|\mathcal{B}_{klt}|}{|\mathcal{A}_{klt}|}, \tag{23}$$

where c_t is the number of all possible configurations of t, and o_t is the number of elements in the orbit of the solution x_i under the action S_n on the set of nonnegative integer solutions of (19). The outer sum ranges over all possible configurations of k sources and l relays from which to destination data transmissions fails. The inner sum ranges over the orbits of the action of S_n on the set of nonnegative integer solutions of (19) or over the orbits of the action of S_n on the set $\{\mathcal{M}_{x_1,x_2,\ldots,x_n}\}$. That is, the inner sum ranges over $x_1, x_2, \ldots, x_n$ where one solution x_i is chosen arbitrarily in each orbit of the action S_n on the set of nonnegative integer solutions of (19).

It is clear that in each orbit of the action of S_n there is an unique solution of (19) satisfying the condition $x_1 \leq x_2 \leq \cdots \leq x_n$. Thus, orbits correspond the partitions of t. Now take a partition of t. Using the orbit-stabilizer theorem (use, for instance, [28, Th. 3.19, p. 57]), we see that the number of elements of the orbit containing a partition of t is equal to the index of its stabilizer in S_n. Given a partition $x_1 \leq x_2 \leq \cdots \leq x_n$ of t, its stabilizer is the set of permutations $\alpha \in S_n$ such that $\alpha(u) = v \iff x_u = x_v$. Letting p be the partition of t we consider and $F(p)$ be the set $\{f \mid x_f \neq x_{f+1}\} \cap \{1, 2, .., n-1\}$, we see that the order of the stabilizer of p is given as:

$$f_1!(f_2 - f_1)!(f_3 - f_2)! \cdots (f_q - f_{q-1})!(n - f_q)!, \tag{24}$$

where $F(p) = \{f_1 < f_2 < \cdots < f_q\}$. Therefore,

$$o_t = \frac{n!}{f_1!(f_2-f_1)!(f_3-f_2)! \cdots (f_q-f_{q-1})!(n-f_q)!}, \tag{25}$$

where for given a partition $p = x_1 \leq x_2 \leq \cdots \leq x_n$ of t, $x(p)$ is defined as follows:

$$x(p) := f_1!(f_2-f_1)!(f_3-f_2)! \cdots (f_q-f_{q-1})!(n-f_q)!. \tag{26}$$

We give a numerical example to explain the action of the symmetric group on the set of solutions and its orbits in the Appendix. Hence, the conditional successful decoding probability (23) is updated as:

$$P(d\ |k\ \text{sd},\ l\ \text{rd},\ t\ \text{sr}) = \sum_{k,l} \frac{1}{c_k c_l} \sum_{p \in \wp_n(t)} \frac{\frac{n!}{x(p)} C(p)}{c_t} \frac{|\mathcal{B}_{klt}|}{|\mathcal{A}_{klt}|}, \tag{27}$$

where the outer sum ranges over all possible configurations of k and l. Here $\wp_n(t)$ denotes the set of nonnegative integer solutions of (19) satisfying $x_1 \leq x_2 \leq \cdots \leq x_n$. Moreover, if $p = x_1 \leq x_2 \leq \cdots \leq x_n$ then

$$C(p) = \frac{m!}{x_1!x_2! \cdots x_n!(m-t)!}. \tag{28}$$

We note that if the action of S_n sends a solution x_i to a solution $\overline{x}_i$ then

$$C(x_1, x_2, \ldots, x_n) = C(\overline{x}_1, \overline{x}_2, \ldots, \overline{x}_n). \tag{29}$$

Thus (21) becomes,

$$c_t = \sum_{p' \in \wp_n(t)} \frac{n!}{x(p')} C(p'). \tag{30}$$

Note that c_t depends only on the values of the numbers k and l, and it does not depend on how k and l are configured. As permuting all the rows of $\mathbf{D}$ and the rows of $\mathbf{R}$ do not change the rank of the block matrix $\mathbf{Z}$, it is clear that the inner sum in (27) does not depend on the particular configurations of k and l. Therefore, (27) is a sum of $c_k c_l$ terms each of which is the same. Since each summand is equal to $\frac{1}{c_k c_l}$ times the inner sum, we see that

$$\begin{aligned} P(d\ |k\ sd,\ l\ rd,\ t\ sr) &= \sum_{p \in \wp_n(t)} \frac{\frac{n!}{x(p)} C(p)}{c_t} \frac{|\mathcal{B}_{klt}|}{|\mathcal{A}_{klt}|} \\ &= \sum_{p \in \wp_n(t)} \frac{\frac{n!}{x(p)} C(p)}{\sum_{p' \in \wp_n(t)} \frac{n!}{x(p')} C(p')} \frac{|\mathcal{B}_{klt}|}{|\mathcal{A}_{klt}|}. \end{aligned} \tag{31}$$

The above expressions about sr link failures are described for the global encoding matrix $\mathbf{Z}$. To reduce computational complexity, we explore the full rank probability of $\mathbf{B}$ as defined in (12). Regarding this which is aforementioned. Hence, the corresponding size of $\mathbf{B}$ is considered for each transmission case when calculating the successful decoding probability of RNCC.

By using the previously defined expressions, the successful decoding probability of RNCC is given in (32), as shown at the top of the next page. This formula depends only on the values of the numbers k and l, and it does not depend on how k and l are configured. Thus, to calculate $|\mathcal{A}_{klt}|$ and $|\mathcal{B}_{klt}|$ may assume that the first k diagonals of $\mathbf{D}$ are zero and the last l rows of $\mathbf{R}$ are zero rows which is stated aforementioned. Note

$$P_d = \sum_{k,l,t} P(d \mid k\ sd,\ l\ rd,\ t\ sr) P_{sd}(k) P_{rd}(l) P_{sr}(t)$$
$$= \sum_{k=0}^{n} \sum_{l=0}^{m-k} \sum_{t=0}^{m-l} \sum_{p \in \wp_n(t)} \left[\frac{\frac{n!}{x(p)} C(p)}{c_t} \frac{|\mathcal{B}_{klt}|}{|\mathcal{A}_{klt}|} \binom{n}{k} \phi_{sd}^k (1-\phi_{sd})^{n-k} \binom{m}{l} \phi_{rd}^l (1-\phi_{rd})^{m-l} \binom{m-l}{t} \right]$$
$$\times \left[\left(\frac{k\phi_{sr}}{n} \right)^t \left(1 - \left(\frac{k\phi_{sr}}{n} \right) \right)^{m-l-t} \right]. \tag{32}$$

$$P_d = \sum_{k=0}^{n} \sum_{l=0}^{m-k} \sum_{t=0}^{m-l} \left[\binom{n}{k} \binom{m}{l} \binom{m-l}{t} \phi_{sd}^k (1-\phi_{sd})^{n-k} \phi_{rd}^l (1-\phi_{rd})^{m-l} \left(\frac{k\phi_{sr}}{n} \right)^t \left(1 - \left(\frac{k\phi_{sr}}{n} \right) \right)^{m-l-t} \right]$$
$$\times \left[\sum_{p \in \wp_n(t)} \frac{\frac{n!}{x(p)} C(p)}{\sum_{p' \in \wp_n(t)} \frac{n!}{x(p')} C(p')} \frac{\left(\mathrm{mat}_q(m-l, k, \hat{S}_{p,1}, k) \right)}{\sum_{r=0}^{k} \mathrm{mat}_q(m-l, k, \hat{S}_p, r)} \right], \tag{34}$$

$$P_d \geq P_d^b = \sum_{k=0}^{n} \sum_{l=0}^{m-k} \left[\binom{n}{k} \binom{m}{l} \phi_{sd}^k (1-\phi_{sd})^{n-k} \phi_{rd}^l (1-\phi_{rd})^{m-l} \left(1 - \left(\frac{k\phi_{sr}}{n} \right) \right)^{m-l-1} \right]$$
$$\times \left\{ \left(1 - \frac{k\phi_{sr}}{n} \right) \sum_{p \in \wp_n(0)} \frac{\frac{n!}{x(p)} C(p)}{\sum_{p' \in \wp_n(0)} \frac{n!}{x(p')} C(p')} \frac{\left(\mathrm{mat}_q(m-l, k, \hat{S}_{p,1}, k) \right)}{\sum_{r=0}^{k} \mathrm{mat}_q(m-l, k, \hat{S}_p, r)} \right.$$
$$\left. + (0.5)^k \sum_{p \in \wp_n(1)} \frac{\frac{n!}{x(p)} C(p)}{\sum_{p' \in \wp_n(0)} \frac{n!}{x(p')} C(p')} \frac{\left(\mathrm{mat}_q(m-l, k, \hat{S}_{p,1}, k) \right)}{\sum_{r=0}^{k} \mathrm{mat}_q(m-l, k, \hat{S}_p, r)} \right\}. \tag{35}$$

that if $l > m-k$ then $m-l < k$ and so $|\mathcal{B}_{klt}| = 0$. That is why the index l of the second sum (32) is from 0 to $m-k$.

The numbers $|\mathcal{A}_{klt}|$ and $|\mathcal{B}_{klt}|$ can be found with using $\mathrm{mat}_q(\cdot)$ functions [29]. In [29], the calculation of number of matrices with a given rank condition is considered while positions of zeros (S) are fixed over a finite field. For fixed positions, these matrices are not defined in polynomials for all cases. In [29, Th. 3.6] it is proven that the problem is a polynomial if the same line is at most two zeros. The defined problem yields this constraint. For any integers m, n, r, and for any subset S, $\mathrm{mat}_q(m, n, S, r)$ is the number of $m \times n$ matrices over $\mathcal{GF}(q)$ of rank r whose $(i, j)^{\text{th}}$ entry is zero if (i, j) is in S [29].

For a fixed partition, $p \in \wp_n(t)$, $|\mathcal{A}_{klt}|$ and $|\mathcal{B}_{klt}|$ can be calculated as:

$$|\mathcal{A}_{klt}| = \sum_{r=0}^{k} \mathrm{mat}_q(m-l, k, \hat{S}_p, r),$$
$$|\mathcal{B}_{klt}| = \mathrm{mat}_q(m-l, k, \hat{S}_{p,1}, k). \tag{33}$$

Therefore, $|\mathcal{A}_{klt}|$ is equal to the number of elements of the set of $(m-l) \times k$ matrices whose t rows contain entries which are forced to zero and whose columns contain these t zeros according to the permutation $p \in \wp_n(t)$. Moreover, $|\mathcal{B}_{klt}|$ is equal to the number of elements of the set of $(m-l) \times k$ matrices, $\mathbf{B}$ with rank k, whose first t rows may contain entries which are forced to zero and whose columns contain these (possibly less than t) zeros according the first k terms of the partition $p \in \wp_n(t)$.

Recalling the assumptions on the configurations of the positions of k, l and t. matrices in $\mathcal{A}_{klt}$ are the block matrices of type $\mathbf{Z}'$, in (12). Thus, a block matrix $\mathbf{Z}'$ in $\mathcal{A}_{klt}$ will be in $\mathcal{B}_{klt}$ if and only if the $(m-l) \times k$ submatrix $\mathbf{B}$ of $\mathbf{Z}'$ will have full rank k. Hence, the successful decoding probability of RNCC given in (32) turns into (34), as shown at the top of this page, where $\hat{S}_p$, and $\hat{S}_{p,1}$ specify respectively the coordinates of the entries that are forced to zero according the partition p, the first k terms of the partition p, and the last $n-k$ terms of the partition p.

The number of source to relay link outages, t, can be less than or equal to $m-l$, as deduced from (34). For each t value, the possible all partitions need to be considered to calculate the exact decoding probability of RNCC. Instead of calculation of full rank matrices over all possible t values, a lower bound for the theoretical successful decoding probability over $t \leq 1$ is given in (35), as shown at the top of this page.

This bound can be used to estimate P_d given in (34) for large m and n values. Considering the decoding failure probability $1 - P_d$, by calculating $1 - P_d^b$, we obtain an upper bound. The validity of the upper bound expression will be explored by comparing the simulation results of RNCC in Section IV.

D. Relay Operations

In this section, we investigate the results of relay operations on successful decoding probability in wireless networks. Instead of using all relays to aid the communication between source-destination pairs, single relay can be selected to satisfy the rank condition at the destination node. We also propose a relay selection scheme to use cooperative diversity without using all relay nodes, which is a standard technique in relay-aided systems in wireless networks [30]. If there are more

than one link failure of sd pairs, aid of a single relay can not cover the rank condition at the destination node. Hence, the single relay selection scheme provides performance gain for only one link failure of sd links. We derive the simplified successful decoding probability expressions for a single relay and single relay selection cases in this subsection.

Firstly, we derive the successful decoding probability expression of single relay case ($m = 1$) which is a commonly seen transmission scheduling in wireless networks due to simplicity of implementation. The single relay case makes the expressions much simpler. The successful decoding probability of a single relay case is given in (36), as shown at the bottom of this page. The single relay has only the capable of increase the rank of $\mathbf{Z}$ up to one extra.

Secondly, we choose a non-outage relay for the corresponding source node which is in outage of sd link to increase the rank of $\mathbf{Z}$. Successful decoding probability expression of single relay selection scheme is given in (37), as shown at the bottom of this page, where $P(d|k\ sd, l\ rd, t\ sr)$ indicates the probability of an increasing in rank of $\mathbf{Z}$ when an sd link fails.

IV. Numerical Results

We give extensive simulation results supporting theoretical results with respect to different system parameters as q, γ_{sd}, γ_{sr}, γ_{rd}, m, and n. We consider up to 4 source and relay nodes ($m, n \in \{1, 2, 3, 4\}$) and also investigate the bound in (35) by considering $m, n \in \{10, 15\}$. The successful decoding probability of RNCC is calculated as per (34) and results are also verified by Monte Carlo simulations.

Firstly, we investigate the effect of field size, q on the decoding failure probability $1 - P_d$ with considering different number relay nodes given in Fig. 2. The theoretical and simulation results overlap and through this figure, we deduce important outcomes about RNCC performance. For the symmetric scenario, SNR values of sd, sr and rd links are kept equal to 5 and 10 dB and two source nodes are considered. Setting the SNR of all links the same value, assists evaluating the effects of the number of relay nodes on failure probability. The increase of q results in improving decoding probability performance for all m values. While the number of relay nodes increases, lower decoding failure probability levels are obtained thanks to the increasing the probability of $\mathbf{Z}$ being full rank. If γ is set to 10 dB, lower failure performances can be obtained over varying q values. The other interesting result of this figure is error floor formed at high q values. The single relay ($m = 1$) result defines the worst case in relay usage perspective as also shown in this figure.

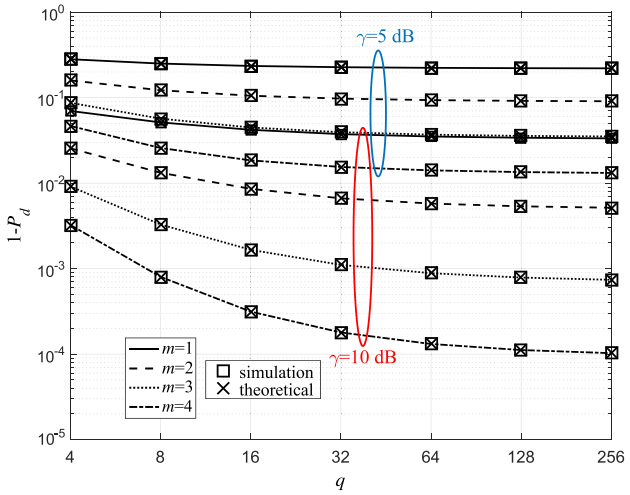

Fig. 2. The decoding failure probability of RNCC, with respect to changing number of relay nodes, m, and field size, q for fixed $n = 2$.

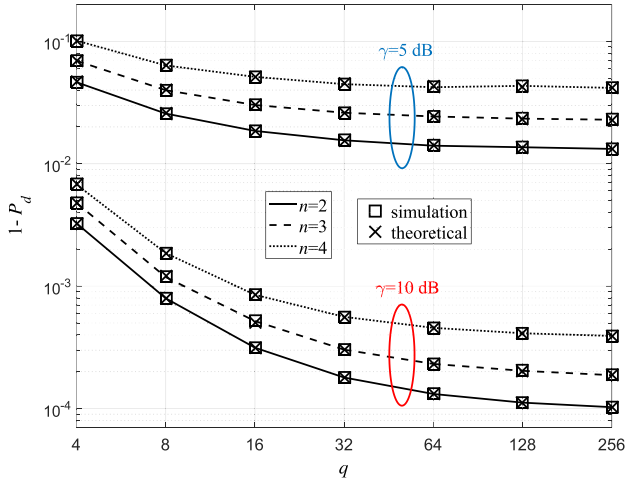

Fig. 3. The decoding failure probability results of RNCC, with respect to changing number of source nodes, n, and field size, q, when $m = 4$.

The number of source nodes, n, is an observable design parameter since the required rank of $\mathbf{Z}$ to successfully decode the received packets at the destination node is equal to n. The performance results about the number of source nodes on successful decoding probability are shown in Fig. 3 with fixed number of relay nodes. If the system consists of more source nodes, the number of columns of $\mathbf{Z}$ will increase, meaning that the rank condition of successful decoding, n, increases. This situation causes decrease in successful decoding probability performance. This is consistent with the numerical

$$P_d = \sum_{k=0}^{1}\sum_{l=0}^{1-k}\sum_{t=0}^{1-l}\left[\binom{n}{k}\phi_{sd}^{k}(1-\phi_{sd})^{n-k}\phi_{rd}^{l}(1-\phi_{rd})^{1-l}\left(\frac{k\phi_{sr}}{n}\right)^{t}\left(1-\left(\frac{k\phi_{sr}}{n}\right)\right)^{1-l-t}\right]\times\left(1-\left(\frac{1}{q}\right)^{1-l-t}\right)^{k}, \tag{36}$$

$$P_d = \sum_{k=0}^{1}\sum_{l=0}^{m-k}\binom{n}{k}\binom{m}{l}\phi_{sd}^{k}(1-\phi_{sd})^{n-k}\phi_{rd}^{l}(1-\phi_{rd})^{m-l}\times\left(1-\sum_{t=0}^{m-l}\binom{m-l}{t}\left(\frac{k\phi_{sr}}{n}\right)^{t}\left(1-\frac{k\phi_{sr}}{n}\right)^{m-l-t}\left(\left(\frac{1}{q}\right)^{m-l-t}\right)^{k}\right), \tag{37}$$

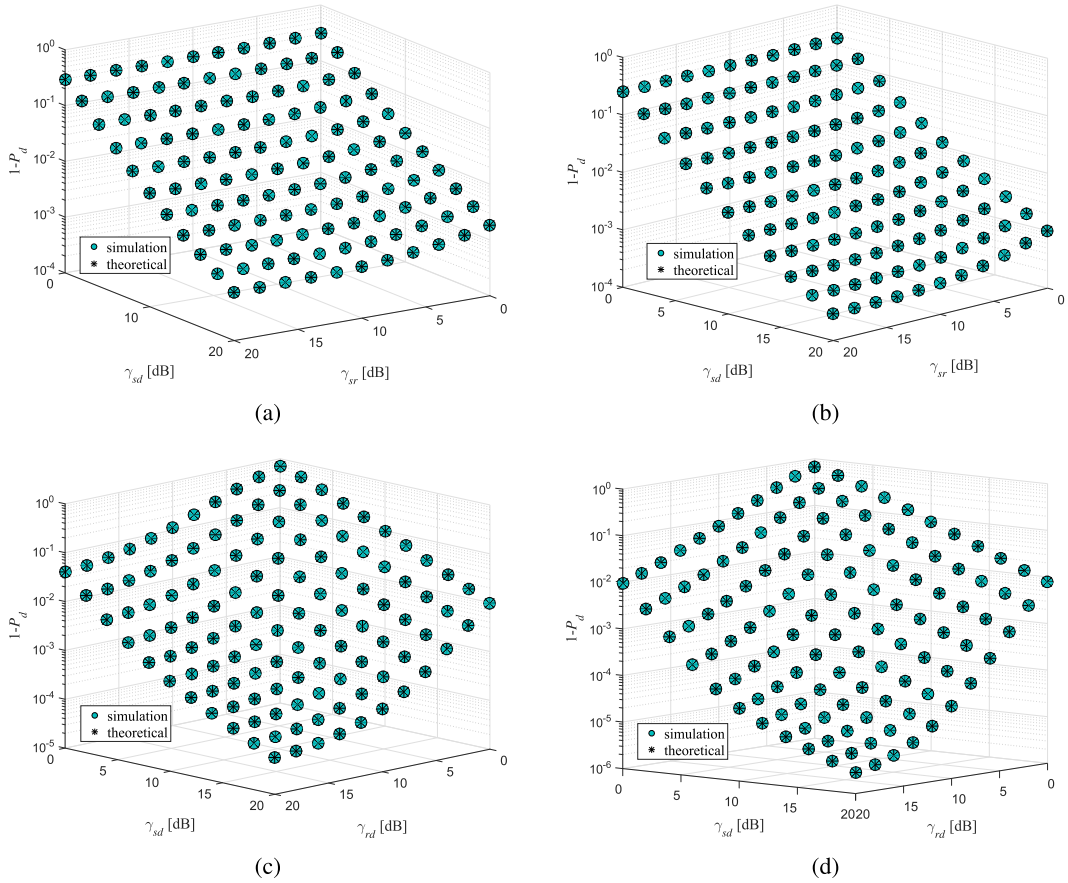

Fig. 4. The decoding failure probabilities of RNCC (a) with respect to SNR of sd and sr links $q = 8$ and $\gamma_{rd} = 5$ dB (b) with respect to SNR of sd and sr links when $q = 64$ and $\gamma_{rd} = 5$ dB (c) with respect to SNR of sd and rd links when $q = 8$ and $\gamma_{sr} = 5$ dB (d) with respect to SNR of sd and rd links when $q = 64$ and $\gamma_{sr} = 5$ dB.

and simulation results. Highest successful decoding probability performance is obtained when $n = 2$ for both of $\gamma = 5$ dB and $\gamma = 10$ dB. The performance is decreasing with increasing number of source nodes. On the other hand, the increasing field size, q, improves successful decoding probability performance for all cases due to the increasing probability of $\mathbf{Z}$ having full rank. On the other hand, if q is sufficiently large, the performance does not improve and the error floors can be encountered. The all results of $\gamma = 5$ dB and $\gamma = 10$ dB also show that the increase in SNR results in performance improvement as expected.

We assume symmetric channel condition to accurately investigate the impacts of m, n, and q on successful decoding probability for various schemes in the previous figures. On the other hand, this assumption may not be reasonable for wireless networks with channel impairments. Hence, we give detailed performance results versus different values of γ_{sd}, γ_{sr} and γ_{rd} in a similar manner in Fig. 4.

Firstly, we explore the results of simultaneous changes in γ_{sd} and γ_{sr} values in Fig. 4 (a) and 4 (b) for $q = 8$ and $q = 64$, respectively. γ_{rd} is assumed to be constant and equal to 5 dB. We easily observe that large γ_{sd} values considerably improve the successful decoding probability performance when compared to small γ_{sd} values for constant γ_{sr} values as can be deduced from both figures. For example, in case of $\gamma_{sd} = 0$ dB and $\gamma_{sr} = 0$ dB, we get the error level of 3×10^{-1}, but if $\gamma_{sd} = 20$ dB and $\gamma_{sr} = 0$ dB, the error is equal to 1.8×10^{-3}. On the contrary, in case of $\gamma_{sd} = 0$ dB and $\gamma_{sr} = 20$ dB, the performance improvement is negligible when compared to the setting when $\gamma_{sd} = 0$ dB and $\gamma_{sr} = 0$ dB. This means that, γ_{sd} has more impact than γ_{sr} on the successful decoding probability.

The effects of joint changes in γ_{sd} and γ_{rd} are taken into account in Fig. 4 (c) and Fig. 4 (d) while $\gamma_{sr} = 5$ dB. The value of q is fixed to 8 and 64, in Fig. 4 (c) and Fig. 4 (d), respectively. Both γ_{sd} and γ_{rd} have important influences on the successful decoding probability which is clearly shown in the figures. If we carefully analyze these figures, γ_{sd} is a slightly more impact than γ_{rd} and this difference disappears for high values of γ_{sd} and γ_{rd}. The larger field size improves successful decoding probability performance which can be observed from Fig. 4 (c) and Fig. 4 (d).

The numerical results of the decoding failure probability analysis for high values of m and n with $q = 2$, $\gamma_{sr} = 20$ dB are shown in Fig. 5. The upper bound ($(1 - P_d^b)$ where P_d^b is given in (35)) closely approximates the simulation results as can be observed from the figure. In the case of $m = n = 10$, the upper bound provides a tight approximation to simulation

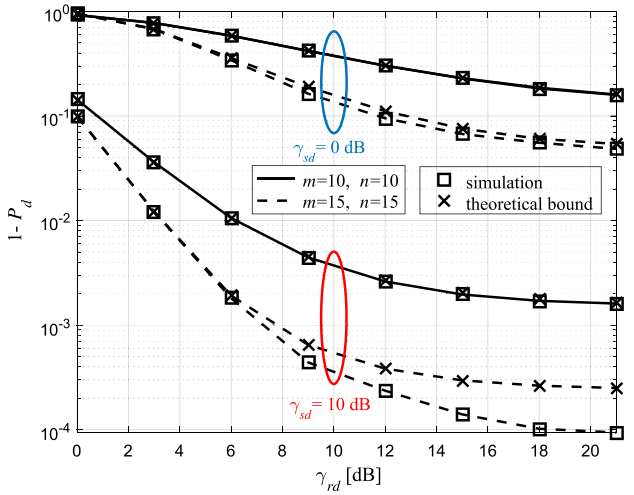

Fig. 5. The upper theoretical bounds ($t \leq 1$) and simulation results of decoding failure probability for $q = 2$ and $\gamma_{sr} = 20$ dB over various m, n, and γ_{sd} values.

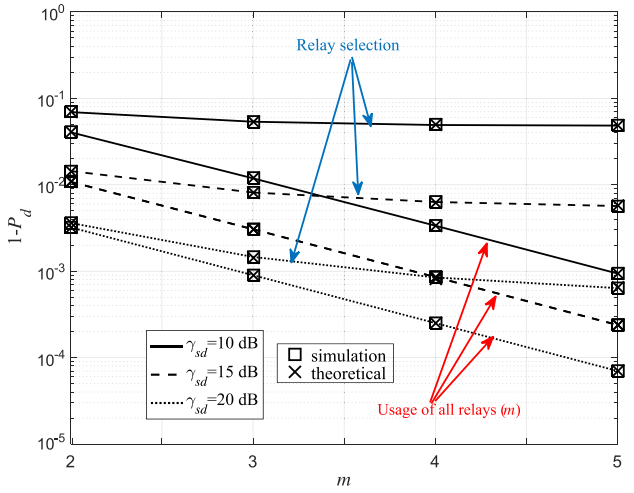

Fig. 6. The decoding failure probability results of relay selection versus m values for varying γ_{sd} for $n = 4$, $q = 4$, $\gamma_{sr} = \gamma_{rd} = 15$ dB.

results for both $\gamma_{sd} = 0$ and $\gamma_{sd} = 10$ dB. When $m = n = 15$, the upper bound closely approximates simulation results only for $\gamma_{sd} = 0$ dB. On the other hand, for $\gamma_{sd} = 10$ dB, the upper bound of decoding failure probability becomes loose as the impact of terms with $t \geq 2$ becomes more apparent.

The last performance analysis contains the single relay selection case. The decoding failure probability results are obtained versus m values for different γ_{sd} values which are given in Fig. 6. We take the fixed values of $m = 4$, $q = 4$, $\gamma_{sr} = 15$ dB and $\gamma_{rd} = 15$ dB. With increasing number of relays, the successful decoding probability performance considerably improves for all the values of γ_{sd}. For high γ_{sd} values, satisfying the full rank condition is more probable than the low values. Hence, the performance improvement due to high γ_{sd} values is apparent for varying m values.

V. Measurement Results

A testbed was designed and created for the real-time implementation of the proposed RNCC model to observe

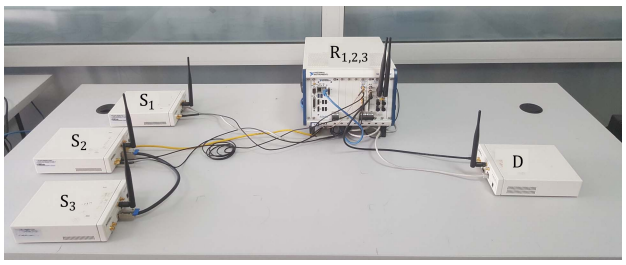

Fig. 7. Implementation setup of RNCC.

performance from a different perspective and validate analytical results. We set up a real-time RNCC testbed to measure decoding probability for single relay case ($m = 1$) with three source nodes ($n = 3$) as shown in Fig. 7.

RNCC testbed is implemented with 4 NI USRP-2921 SDR nodes, where three of them are used as source nodes and the fourth node is used as the destination. The distance between relay and source (destination) nodes (node) pairs are equal to around 1 m (50 cm). For relay node, NI PXIe-5644R Vector Signal Transceiver (VST) module is utilized which can operate in 65 MHz to 6 GHz frequency range and can support 80 MHz instantaneous bandwidth. Moreover, NI PXI-6683H timing and synchronization module, which includes a TCXO oscillator, is used as the synchronization source. All modules are managed via NI PXIe-1082 chassis. LabVIEW is used as the software tool.

QPSK is used as the modulation scheme at all nodes. To satisfy the orthogonality principle of transmissions, we use orthogonal frequency division multiple access (OFDMA) technique. The coding coefficients are selected from $\mathcal{GF}(4)$ $i.i.d.$ with uniformly distributed. We obtain the outage probability results of transmission links by using pilot symbols as pseudo-noise (PN) sequences [31]. According to this, symbols are demodulated to bits and each bit sequence of the source node is compared with transmitted bit sequence. With the corresponding input-output configurations, RNCC-OFDMA system is realized.

We simplify the expressions by using three types of channel assumption (γ_{sd}, γ_{sr}, γ_{rd}), also named as symmetric case, in the previous sections. On the other hand, we also observe the results of relaxing this assumption, defined as asymmetric case, for sd links are shown in Fig. 8 with $m = 3$, $n = 3$. Although there is physically a single relay node, it uses frequency division multiple access principles to behave as three relay nodes and transmits three random network coded symbols. In this figure, we investigate both of the effects of the asymmetric case of sd links and real-time test results. Firstly, the solid line indicates the symmetric case implying that all sd links has the same SNR, $\gamma_{s_jd} = \gamma'_{sd}$. The dashed line denotes the results of the asymmetric case with constant 5 dB difference, where $\gamma_{s_1d} = \gamma'_{sd} - 5$ dB, $\gamma_{s_2d} = \gamma'_{sd}$ dB, and $\gamma_{s_3d} = \gamma'_{sd} + 5$ dB γ'_{sd} is equal to mean value of γ_{s_1d}, γ_{s_2d}, and γ_{s_3d}. The asymmetric case has only a small performance penalty of 1 dB while $\gamma'_{sd} = 10$ dB compared to the symmetric case. We obtain five distinct measurement sets form our testbed refer to as Test-M1, Test-M2, Test-M3, Test-M4, and Test-M5. The average estimated SNR values of

TABLE I
MEASUREMENT RESULTS OF THE TESTBED ARE USED IN FIG. 8.

	Test-M1	Test-M2	Test-M3	Test-M4	Test-M5
Transmit Gain [dB]	6	9	11	16	18
$\gamma_{s_1 d}$ [dB]	5.9	8.27	8.8	12.8	14.6
$\gamma_{s_2 d}$ [dB]	6.6	8.87	9.4	13.6	14.3
$\gamma_{s_3 d}$ [dB]	8.1	9.53	10	13.5	15.4

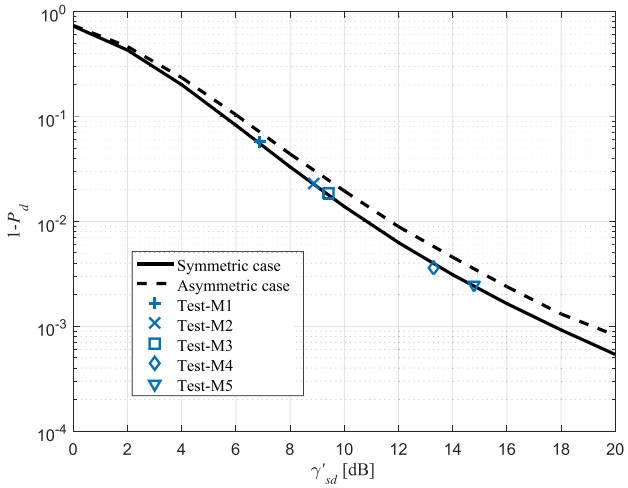

Fig. 8. The decoding failure probability results of tests with simulations versus mean SNR value of sd links, γ'_{sd}, where m, and n are equal to 3.

each measurement are given in Table I. We obtain various SNR results of the measurements due to the effect of different transmit gains of source nodes.

The test results show that the qualities of different links may be different according to environmental factors. Although SNR values of each sd link are different from each other, the performance results of these cases are very close to the symmetric case, which is shown in Fig. 8.

VI. CONCLUSION

The extensive successful decoding performance analyses of RNCC are presented for various cooperative transmission schemes in wireless networks. The theoretical successful decoding probability results of RNCC has been derived for a generalized multi-source and multi-relay system. In addition to generalized transmission scheme, the results of single relay and single relay selection cases have been also presented. The reliability of the given theoretical results has been supported through extensive simulation results. Both the theoretical and simulation results are compatible with each other highlights the contribution of the paper. The RNCC testbed which is established with SDR nodes have been also presented. The obtained measurement results emphasize the validity and the practicality of the theoretical results.

As future work, we target to investigate the impact of sparsity in RNC in densely populated network scenarios and quantify the impact of relay selection techniques. We also target to apply RNC to different applications, specifically for storage and content distribution, taking the associated application requirements into consideration.

APPENDIX
AN EXAMPLE OF ORBIT COUNTING

We give an example to explain the action of the symmetric group on the set of solutions and on columns of matrices, and its orbits. Assume that there are $n = 3$ sources and $m = 4$ relays. For $t = 3$, three rows of the 4×3 matrix $\mathbf{R}$ given in (8) have (exactly one) forced zeros. How these forced zeros are distributed among the columns of $\mathbf{R}$ corresponds to the nonnegative integer solutions of the equation $x_1+x_2+x_3 = 3$, where x_j denotes the number of forced zeros in the j^{th} column of $\mathbf{R}$. The number of such solutions is $\binom{3+3-1}{3} = 10$. They are

$$\begin{aligned}&(x_1, x_2, x_3)\\ &= (3,0,0),\ (0,3,0),\ (2,1,0),\ (0,0,3),\ (2,0,1),\\ &\quad (0,2,1),\ (1,2,0),\ (0,1,2),\ (1,0,2),\ (1,1,1).\end{aligned} \tag{38}$$

The symmetric group of order 3! acts on this set by permuting the solutions. For instance, this action transforms the solution $(0, 1, 2)$ to $(2, 0, 1)$. This means in particular that the solutions $(0, 1, 2)$ and $(2, 0, 1)$ are in the same orbit. We see that the orbits are the following three sets

$$\begin{aligned}&\{(3,0,0),(0,3,0),(0,0,3)\},\\ &\quad \{(2,1,0),(2,0,1),(0,2,1),(1,2,0),(1,0,2),(0,1,2)\},\\ &\quad \{(1,1,1)\}.\end{aligned} \tag{39}$$

Note that the set of all solutions is the disjoint union of these orbits. In each orbit, there is a unique solution such that $x_1 \le x_2 \le x_3$. So each orbit corresponds to a partition of 3. For instance, the first orbit corresponds to the partition $(0, 0, 3)$, the second orbit corresponds to the partition $(0, 1, 2)$, and the third orbit corresponds to the partition $(1, 1, 1)$. To calculate the number of elements of each orbit we need to calculate the index of the stabilizer of each of these partitions. Note that a permutation fixes $(0, 0, 3)$ if and only if it does not move the third solution $x_3 = 3$ (but it may interchange the first two solutions x_1 and x_2). Thus, the stabilizer of $(0, 0, 3)$ has 2! elements. Therefore the number of elements of the orbit containing $(0, 0, 3)$ is $\frac{3!}{2!} = 3$. This number corresponds the expression $\frac{n!}{x(p)}$. Consider the partition $p = (0, 0, 3)$, so that $x_1 = 0, x_2 = 0, x_3 = 3$. Then

$$F(p) = \{f | x_f \neq x_{f+1}\} \cap \{1, 2\} = \{2\}. \tag{40}$$

$$\left[\begin{array}{|c|c|c|}\hline 0 & & \\ \hline 0 & & \\ \hline & & 0 \\ \hline\end{array}\right], \left[\begin{array}{|c|c|c|}\hline 0 & & \\ \hline 0 & & \\ \hline & & 0 \\ \hline\end{array}\right], \left[\begin{array}{|c|c|c|}\hline 0 & & \\ \hline & & 0 \\ \hline 0 & & \\ \hline\end{array}\right], \left[\begin{array}{|c|c|c|}\hline 0 & & \\ \hline & & \\ \hline 0 & & \\ \hline\end{array}\right], \left[\begin{array}{|c|c|c|}\hline 0 & & \\ \hline & & 0 \\ \hline 0 & & \\ \hline\end{array}\right], \left[\begin{array}{|c|c|c|}\hline 0 & & \\ \hline & & \\ \hline & & 0 \\ \hline\end{array}\right]$$

$$\left[\begin{array}{|c|c|c|}\hline & & 0 \\ \hline 0 & & \\ \hline 0 & & \\ \hline\end{array}\right], \left[\begin{array}{|c|c|c|}\hline & & \\ \hline 0 & & \\ \hline 0 & & \\ \hline\end{array}\right], \left[\begin{array}{|c|c|c|}\hline & & 0 \\ \hline 0 & & \\ \hline & & \\ \hline\end{array}\right], \left[\begin{array}{|c|c|c|}\hline & & \\ \hline 0 & & \\ \hline & & 0 \\ \hline\end{array}\right], \left[\begin{array}{|c|c|c|}\hline & & 0 \\ \hline & & \\ \hline 0 & & \\ \hline\end{array}\right], \left[\begin{array}{|c|c|c|}\hline & & \\ \hline & & 0 \\ \hline 0 & & \\ \hline\end{array}\right]. \tag{43}$$

Hence $F(p) = \{f_1\}$ with $f_1 = 2$ where $q = 1$ also, and so

$$\begin{aligned} x(p) &:= f_1!(f_2 - f_1)!(f_3 - f_2)! \cdots (f_q - f_{q-1})!(n - f_q)! \\ &= 2!(3-2)!, \end{aligned} \tag{41}$$

and so the orbit has $\frac{n!}{x(p)} = \frac{3!}{2!(3-2)!} = 3$ elements.

Now let us explain the action of S_3 on the set $\left\{\mathcal{M}\right\}$. For each solution of $x_1 + x_2 + x_3 = 3$ there is a set in $\left\{\mathcal{M}\right\}$. Indeed, the set is equal to:

$$\begin{aligned} \{\mathcal{M}\} = \big\{&\mathcal{M}_{3,0,0}, \mathcal{M}_{0,3,0}, \mathcal{M}_{0,0,3}, \mathcal{M}_{2,1,0}, \mathcal{M}_{2,0,1}, \mathcal{M}_{0,2,1}, \\ &\mathcal{M}_{1,2,0}, \mathcal{M}_{0,1,2}, \mathcal{M}_{1,0,2}, \mathcal{M}_{1,1,1}\big\}. \end{aligned} \tag{42}$$

For instance, as the action of S_3 on the solutions transforms the solution $(2, 0, 1)$ to the solution $(0, 1, 2)$ it follows that the action of S_3 on $\left\{\mathcal{M}\right\}$ transforms the set $\mathcal{M}_{2,0,1}$ to the set $\mathcal{M}_{0,1,2}$. Therefore, the orbits of the S_3 action on $\left\{\mathcal{M}\right\}$ are the following three sets: $\left\{\mathcal{M}_{3,0,0}, \mathcal{M}_{0,3,0}, \mathcal{M}_{0,0,3}\right\}$, $\left\{\mathcal{M}_{2,1,0}, \mathcal{M}_{2,0,1}, \mathcal{M}_{0,2,1}, \mathcal{M}_{1,2,0}, \mathcal{M}_{0,1,2}, \mathcal{M}_{1,0,2}\right\}$, and $\left\{\mathcal{M}_{1,1,1}\right\}$.

For instance, $\mathcal{M}_{2,0,1}$ is the set of all 4×3 matrices whose rows have at most one forced zeros and whose first column has 2 forced zeros and whose second column has no forced zeros and whose third column has one forced zero. Moreover, $|\mathcal{M}_{2,0,1}| = C(2, 0, 1) = \frac{4!}{2!0!1!(4-3)!} = 12$. Indeed, $\mathcal{M}_{2,0,1}$ consists of the following 12 matrices given in (43), as shown at the top of this page.

We calculate also that

$$\begin{aligned} |\mathcal{M}_{3,0,0}| &= |\mathcal{M}_{0,3,0}| = |\mathcal{M}_{0,0,3}| = 4 \\ |\mathcal{M}_{2,1,0}| &= |\mathcal{M}_{2,0,1}| = |\mathcal{M}_{0,2,1}| \\ &= |\mathcal{M}_{1,2,0}| = |\mathcal{M}_{0,1,2}| = |\mathcal{M}_{1,0,2}| = 12 \\ |\mathcal{M}_{1,1,1}| &= 24. \end{aligned} \tag{44}$$

Therefore, in total there are 108 possible configurations of t which is also indicated by c_t. In this example there are $c_t = 108$ possibilities. If we choose any two sets $\mathcal{M}$ and $\overline{\mathcal{M}}$ from the same orbit of the action of S_3 on $\left\{\mathcal{M}\right\}$ and if we choose any two matrices $\mathbf{M} \in \mathcal{M}$ and $\overline{\mathbf{M}} \in \overline{\mathcal{M}}$, then the number of matrices of rank r of the type of the first matrix $\mathbf{M}$ and the second matrix $\overline{\mathbf{M}}$ are the same. To calculate the numbers $|\mathcal{A}_{klt}|$ and $|\mathcal{B}_{klt}|$ for each possible 108 types, it is enough to consider any one of the matrices in any set in each of the orbit. As the orbit sizes are different, in calculating the successful decoding probability for a fixed $t = 3$, instead of summing over all 108 possibilities, we sum over orbits, so our sum will have 3 summands, but each summand must be multiplied by $\frac{C(x_1, x_2, x_3)N}{108}$ where N is the number of elements in the orbit. To be more precise, letting the orbits be:

$$\begin{aligned} &\{(3, 0, 0), (0, 3, 0), (0, 0, 3)\}, \\ &\quad \{(2, 1, 0), (2, 0, 1), (0, 2, 1), (1, 2, 0), (1, 0, 2), (0, 1, 2)\}, \\ &\quad \{(1, 1, 1)\}, \end{aligned} \tag{45}$$

the success probability at t is calculated as:

$$\sum_{i=1}^{108} \frac{1}{108} \frac{|F_i|}{|Z_i|} = \frac{3C(0,0,3)}{108} \frac{|F|}{|Z|} + \frac{6C(0,1,2)}{108} \frac{|F'|}{|Z'|} + \frac{C(1,1,1)}{108} \frac{|F''|}{|Z''|}. \tag{46}$$

ACKNOWLEDGMENT

The authors would like to thank Joel B. Lewis and Alejandro H. Morales for their support with regard to the implementation of $\mathrm{mat}_q(\cdot)$ function. Computing resources used in this work were partially provided by the National Center for High Performance Computing of Turkey (UHeM).

REFERENCES

[1] R. Ahlswede, N. Cai, S.-Y. R. Li, and R. W. Yeung, "Network information flow," *IEEE Trans. Inf. Theory*, vol. 46, no. 4, pp. 1204–1216, Jul. 2000.

[2] R. W. Yeung, "Multilevel diversity coding with distortion," *IEEE Trans. Inf. Theory*, vol. 41, no. 2, pp. 412–422, Mar. 1995.

[3] S.-Y. R. Li, R. W. Yeung, and N. Cai, "Linear network coding," *IEEE Trans. Inf. Theory*, vol. 49, no. 2, pp. 371–381, Feb. 2003.

[4] C. K. Ngai and R. W. Yeung, "Network coding gain of combination networks," in *Proc. IEEE Inf. Theory Workshop*, Oct. 2004, pp. 283–287.

[5] A. Sendonaris, E. Erkip, and B. Aazhang, "User cooperation diversity. Part I. System description," *IEEE Trans. Commun.*, vol. 51, no. 11, pp. 1927–1938, Nov. 2003.

[6] A. Sendonaris, E. Erkip, and B. Aazhang, "User cooperation diversity. Part II. Implementation aspects and performance analysis," *IEEE Trans. Commun.*, vol. 51, no. 11, pp. 1939–1948, Nov. 2003.

[7] J. N. Laneman, G. W. Wornell, and D. N. C. Tse, "An efficient protocol for realizing cooperative diversity in wireless networks," in *Proc. IEEE ISIT*, Jun. 2001, p. 294.

[8] S. T. Başaran, G. K. Kurt, M. Uysal, and I. Altunbaş, "A tutorial on network coded cooperation," *IEEE Commun. Surveys Tuts.*, vol. 18, no. 4, pp. 2970–2990, 4th Quart., 2016.

[9] R. Koetter and F. R. Kschischang, "Coding for errors and erasures in random network coding," *IEEE Trans. Inf. Theory*, vol. 54, no. 8, pp. 3579–3591, Aug. 2008.

[10] T. Ho, R. Koetter, M. Medard, D. R. Karger, and M. Effros, "The benefits of coding over routing in a randomized setting," in *Proc. IEEE ISIT*, Jun. 2003, p. 442.

[11] P. A. Chou, Y. Wu, and K. Jain, "Practical network coding," in *Proc. Allerton Conf. Commun., Control, Comput.*, Monticello, IL, USA, Oct. 2003, pp. 40–49.
[12] T. Ho *et al.*, "A random linear network coding approach to multicast," *IEEE Trans. Inf. Theory*, vol. 52, no. 10, pp. 4413–4430, Oct. 2006.
[13] C. Khirallah, D. Vukobratović, and J. Thompson, "Performance analysis and energy efficiency of random network coding in LTE-Advanced," *IEEE Trans. Wireless Commun.*, vol. 11, no. 12, pp. 4275–4285, Dec. 2012.
[14] D. Vukobratović, C. Khirallah, V. Stanković, and J. S. Thompson, "Random network coding for multimedia delivery services in LTE/LTE-Advanced," *IEEE Trans. Multimedia*, vol. 16, no. 1, pp. 277–282, Jan. 2014.
[15] O. Trullols-Cruces, J. M. Barcelo-Ordinas, and M. Fiore, "Exact decoding probability under random linear network coding," *IEEE Commun. Lett.*, vol. 15, no. 1, pp. 67–69, Jan. 2011.
[16] C.-F. Chiasserini, E. Viterbo, and C. Casetti, "Decoding probability in random linear network coding with packet losses," *IEEE Commun. Lett.*, vol. 17, no. 11, pp. 1–4, Nov. 2013.
[17] J.-T. Seong, "Bounds on decoding failure probability in linear network coding schemes with erasure channels," *IEEE Commun. Lett.*, vol. 18, no. 4, pp. 648–651, Apr. 2014.
[18] J.-T. Seong and H.-N. Lee, "Predicting the performance of cooperative wireless networking schemes with random network coding," *IEEE Trans. Commun.*, vol. 62, no. 8, pp. 2951–2964, Aug. 2014.
[19] A. S. Khan and I. Chatzigeorgiou, "Improved bounds on the decoding failure probability of network coding over multi-source multi-relay networks," *IEEE Commun. Lett.*, vol. 20, no. 10, pp. 2035–2038, Oct. 2016.
[20] A. S. Khan, A. Tassi, and I. Chatzigeorgiou, "Rethinking the intercept probability of random linear network coding," *IEEE Commun. Lett.*, vol. 19, no. 10, pp. 1762–1765, Oct. 2015.
[21] A. Tassi, I. Chatzigeorgiou, and D. E. Lucani, "Analysis and optimization of sparse random linear network coding for reliable multicast services," *IEEE Trans. Commun.*, vol. 64, no. 1, pp. 285–299, Jan. 2016.
[22] P. J. S. G. Ferreira, B. Jesus, J. Vieira, and A. J. Pinho, "The rank of random binary matrices and distributed storage applications," *IEEE Commun. Lett.*, vol. 17, no. 1, pp. 151–154, Jan. 2013.
[23] A. S. Khan and I. Chatzigeorgiou, "Performance analysis of random linear network coding in two-source single-relay networks," in *Proc. IEEE ICCW*, Jun. 2015, pp. 991–996.
[24] H. Topakkaya and Z. Wang, "Wireless network code design and performance analysis using diversity-multiplexing tradeoff," *IEEE Trans. Commun.*, vol. 59, no. 2, pp. 488–496, Feb. 2011.
[25] M. J. Siavoshani, S. Mohajer, C. Fragouli, and S. N. Diggavi, "On the capacity of noncoherent network coding," *IEEE Trans. Inf. Theory*, vol. 57, no. 2, pp. 1046–1066, Feb. 2011.
[26] M. Siavoshani, S. Yang, and R. Yeung, "Non-coherent network coding: An arbitrarily varying channel approach," in *Proc. IEEE ISIT*, Jul. 2012, pp. 1672–1676.
[27] D. Dummit and R. Foote, *Abstract Algebra*. Hoboken, NJ, USA: Wiley, 2004.
[28] J. J. Rotman, "An introduction to the theory of groups," in *Graduate Texts in Mathematics*. New York, NY, USA: Springer, 1999.
[29] A. J. Klein, J. B. Lewis, and A. H. Morales, "Counting matrices over finite fields with support on skew Young diagrams and complements of rothe diagrams," *J. Algebraic Combinat.*, vol. 39, no. 2, pp. 429–456, 2013.
[30] J. N. Laneman, D. N. C. Tse, and G. W. Wornell, "Cooperative diversity in wireless networks: Efficient protocols and outage behavior," *IEEE Trans. Inf. Theory*, vol. 50, no. 12, pp. 3062–3080, Dec. 2004.
[31] H. M. Mahmoud, A. S. Mousa, and R. Saleem, "Channel estimation based in comb-type pilots arrangement for OFDM system over time varying channel," *J. Netw.*, vol. 5, no. 7, pp. 766–772, 2010.

Semiha Tedik Basaran (S'13) received the B.Sc. and M.Sc. degrees in electronics and communication engineering from Istanbul Technical University, Istanbul, Turkey, in 2011 and 2013, respectively, where she is currently pursuing the Ph.D. degree. She is currently a Research Assistant with Istanbul Technical University. Her primary research interests focus on full-duplex communication, network coding, cooperative communication, and wireless distributed storage systems.

Selahattin Gokceli received the bachelor's degree in electronics and communication engineering from Istanbul Technical University (ITU), Instanbul, Turkey, in 2015, where he is currently pursuing the master's degree in telecommunication engineering. He has been a member of the ITU Wireless Communication Research Laboratory since 2014. He is an NI Certified LabVIEW Associate Developer, and he has used LabVIEW as a programming tool in projects, such as software defined radio implementations of OFDMA-based NCC systems, cooperative communication, and 5G techniques such as full-duplex communication. His current research interests include cooperative communication networks and 5G techniques.

Gunes Karabulut Kurt (M'06–SM'15) received the B.S. degree (Hons.) in electronics and electrical engineering from Bogazici University, Istanbul, Turkey, in 2000, and the M.A.Sc. and Ph.D. degrees in electrical engineering from the University of Ottawa, ON, Canada, in 2002 and 2006, respectively. From 2000 to 2005, she was a Research Assistant with the CASP Group, University of Ottawa. From 2005 to 2006, she was with TenXc Wireless, where she was involved in location estimation and radio-frequency identification systems. From 2006 to 2008, she was with Edgewater Computer Systems Inc., where she was involved in high-bandwidth networking in aircraft and priority-based signaling methodologies. From 2008 to 2010, she was with Turkcell Research and Development Applied Research and Technology, Istanbul. Since 2010, she has been an Associate Professor with Istanbul Technical University. Her current research interests include sparse signal decomposition algorithms, multicarrier networks, traffic analysis, and network planning/management. She is a Marie Curie Fellow.

Enver Ozdemir received the Ph.D. degree in mathematics from the University of Maryland, College Park, MD, USA, in 2009. He is currently an Associate Professor with the Institute of Informatics, Istanbul Technical University. His research interests are cryptography, computational number theory, and network security. He was a member of the Coding Theory and Cryptography Research Group, Nanyang Technological University, Singapore, from 2010 to 2014.

Ergün Yaraneri received the Ph.D. degree in mathematics from Bilkent University in 2008. He is currently an Associate Professor with the Department of Mathematics, Istanbul Technical University. His research interests are representation theory of groups and algebras, number theory, and cryptography.